BENCHMARKING CEASIOM SOFTWARE TO PREDICT FLIGHT CONTROL AND FLYING QUALITIES OF THE B-747

A. Da Ronch*, C. McFarlane, C. Beaverstock**, J. Oppelstrup†, M. Zhang†, A.Rizzi†**
*** Department of Engineering, University of Liverpool, Liverpool, UK**
**** Department of Aerospace Engineering, Bristol University, Bristol, UK**
† Dept. of Aeronautical & Vehicle Engineering,
Royal Institute of Technology (KTH), Stockholm, Sweden

Keywords: *Aircraft design, aerodynamics, flight dynamics, flight control, CFD.*

Abstract

CEASIOM, the Computerized Environment for Aircraft Synthesis and Integrated Optimization Methods, is a framework that integrates discipline-specific tools for conceptual design. At this early stage of the design it is very useful to be able to predict the flying and handling qualities of the aircraft. In order to do this for the configuration being studied, the aerodynamic database needs to be computed and coupled to the stability and control tools to carry out the analysis. This paper describes how the adaptive-fidelity Computational Fluid-Dynamics module of CEASIOM computes the aerodynamic database of an aircraft configuration, and how that data is analyzed by the Flight Control System Designer Toolkit module to determine the flying qualities and the control laws of the aircraft. The paper compares the predicted flying qualities with the flight-test data of the Boeing B747 aircraft in order to verify the goodness of the overall approach.

1 Introduction

There is much current interest in using Computational Fluid-Dynamics (CFD) to compute the static and dynamic forces and moments acting on an aircraft as a complement to the usual practice of measuring them in a wind-tunnel. In verifying the validity of this approach, the usual exercise is to compute the static and dynamic coefficients or derivatives and compare them with the corresponding values measured in the wind tunnel. Such a comparison reveals the differences and similarities between the two approaches, but says little about the sensitivity of the stability and control characteristics to these differences. A further step must be taken to provide insight on the overall accuracy of the CFD predictions of aircraft behaviour in flight. One way is to process the CFD-generated aero-data by linear and nonlinear stability and control analysis and extract flying or handling qualities that can be compared with flight-test data. This is the approach taken in this paper. The tool used to do this is CEASIOM, the Computerized Environment for Aircraft Synthesis and Integrated Optimization Methods, currently being developed within the frame of the SimSAC Project [1], Simulating Aircraft Stability And Control Characteristics for Use in Conceptual Design, sponsored by the European Commission 6th Framework Programme. CEASIOM uses adaptive-fidelity CFD to create the aerodynamic dataset and then uses it to analyze flying qualities using its stability and control analysis tools. The predicted flying qualities of the Boeing B747-100 aircraft are compared to those observed in flight tests [1].

[1] http://www.simsacdesign.eu

2 CEASIOM

CEASIOM [2]is a framework tool that integrates discipline-specific tools comprising Computer-Aided Design (CAD) and mesh generation tools, Computational Fluid-Dynamics (CFD) codes, Stability and Control (S&C) softwares, ..., all for the purpose of aircraft conceptual design [3]. An overview of the CEASIOM environment is provided in Fig. 1. Significant components embodied in CEASIOM are

1. *Geometry module*, Geo–SUMO: a customized geometry construction system that allows users to define the geometry in a XML file by a small number, on the order of hundreds, parameters with intuitive interpretation

2. *Aerodynamic module*, AMB–CFD: uses adaptive fidelity CFD to replace or complement current handbook aerodynamic methods with the steady and unsteady TORNADO Vortex-Lattice Method (VLM) and CFD codes in Euler mode for low speed and high-speed regimes, and support for external RANS (Reynolds Averaged Navier-Stokes) flow simulators for high-fidelity analysis of extreme flight conditions [4]

3. *Stability and Control module*, SDSA: a simulation and dynamic stability and control analyzer and flying-quality assessor; it comprises six degrees of freedom test flight simulation, performance prediction, including human pilot model, Stability Augmentation System (SAS), and a Linear Quadratic Regulator (LQR) based flight control system package [5] among many other features [6]

4. *Aero-elastic module*, NeoCASS: quasi-analytical structural sizing and Doublet-Lattice Method (DLM), finite element model generation [7]; linear aeroelastic analysis and structural optimization [8]; low fidelity panel methods usually adopted

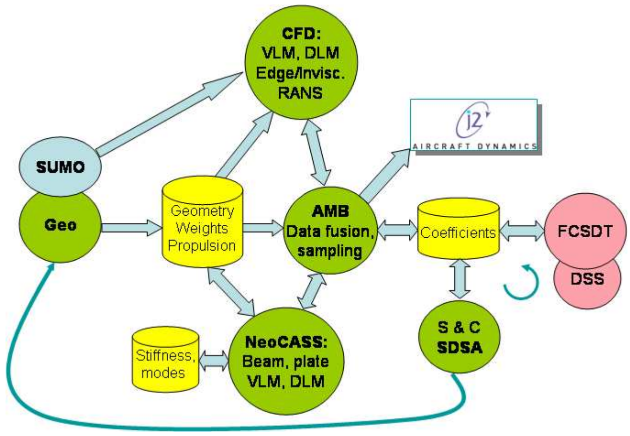

Fig. 1 CEASIOM framework consists of geometry, aerodynamic, structure and stability and control modules

5. *Flight Control System design module*, FCSDT: a designer toolkit for flight control–law formulation, simulation and technical decision support, permitting flight control system design philosophy and architecture to be coupled in the early phase of conceptual design [9]

6. *Decision Support System module*, DSS: an explicit DSS functionality, including issues such as fault tolerance and failure tree analysis [10]

The paper continues with a presentation of the relevant modules involved actively in this study. Emphasis is put on the automated generation of the Euler grid for the B747 model geometry. Aerodynamic sources are revised and a smart procedure to reduce the total number of CFD simulations required to fill-in the aerodynamic tables outlined. Predictions of aerodynamic loads at low and high speed are compared to experimental data. Then, results obtained with the FCSDT software are illustrated.

3 Geometry

The successful generation of aerodynamic tables for flight dynamic applications using high-fidelity CFD tools depends strongly on the system capabilities to create a suitable mesh for the numerical simulation in a reasonable amount of time. Traditionally, the generation of a computational mesh for a new aircraft configuration is an expensive process. During the design phase, the aircraft geometry is often modified iteratively to improve certain aspects or avoid undesiderable aircraft behaviour. The generation of a new mesh at every design iteration, if not automated, would become a bottleneck in the design phase. Citing Dawes et al. [11], the question is "whether CFD can participate in the design process with sufficient speed to drive down the design cycle time". Progress has been made in this direction, as exemplified by the customized geometry modeller for aircraft design, Vehicle Sketch Pad [12], which supports export of meshable surface models and/or meshes in standard formats such as IGES, STEP, and CGNS.

3.1 SUMO

A very attractive feature of the CEASIOM framework is offered by the SUrface MOdeler, referred to as SUMO [13], for the rapid generation of three-dimensional, watertight aircraft geometries that are adequate for high-fidelity analysis using CFD. SUMO [2] is a graphical tool aimed at rapid creation of aircraft geometries and automatic surface mesh generation. It is not a full-fledged CAD system, but rather a easy-to-use sketchpad, highly specialized towards aircraft configurations. SUMO is based on a C++ library for geometric primitives such as b-spline surfaces, and currently provides a graphical frontend to a small subset of the library. It is actively developed in order to streamline the workflow as far as possible to the intended use: rapid surface modelling of aircraft configurations. Unstructured surface meshes can be generated completely without user intervention. Heuristics determine default parameters for the mesh generation code, which usually yield a satisfactory mesh. Manual tuning of these parameters is possible as well. Triangulations are based on a three-dimensional in-sphere criterion, which yields better mesh quality than Delaunay methods for strongly skewed surfaces, such as thin, swept delta-wings. Geometric refinement criteria produce a finer mesh in regions of strong curvature, while a limit on the minimum element size can be imposed to avoid resolution of irrelevant geometric detail. Unstructured volume meshes can be generated from the surface mesh, using the tetrahedral mesh generator TetGen [14]. The volume mesh can be saved as CGNS, a bmsh file for the CFD solver EDGE [15], or TetGen's plain ASCII format.

Unstructured Euler grids for different deflection of the canard wing were generated using SUMO for the investigation of aerodynamic characteristics of a TRansonic Cruise, TCR, wind tunnel model [16]. A recent study [17] presented a viable route to generate high-quality RANS grids using SUMO . The approach used in this study stems from the geometry aircraft definition based on the CEASIOM XML file. The representative geometry of the B747 model is illustrated in Fig. 2(a). The description is used to generate a triangular mesh on the surface, and at the next level, the volume mesh is generated using tetrahedral elements filling the space between the wall and the farfield. This is shown in Fig. 2(b).

4 Aerodynamics

A prerequisite for realistic prediction of the stability and control behaviour of an aircraft is the availability of complete and accurate aerodynamic data. Traditionally, wind-tunnel measurements are used to fill look-up tables of forces and moments over the flight envelope. These wind-tunnel models only become available late in the design cycle. To date, most engineering tools for aircraft design rely on handbook methods or linear fluid mechanics assumptions. These methods provide low cost reliable data as long as the aircraft remains well within the limits of the flight envelope. However, current trends in aircraft design towards augmented-stability and expanded flight envelopes require an accurate description of the non-linear flight-dynamic behaviour of the aircraft. CFD can be used as complement and

[2] http://www.larosterna.com/dwfs.html

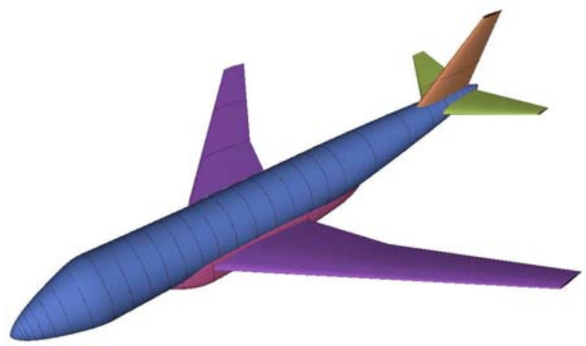

(a) SUMO geometry

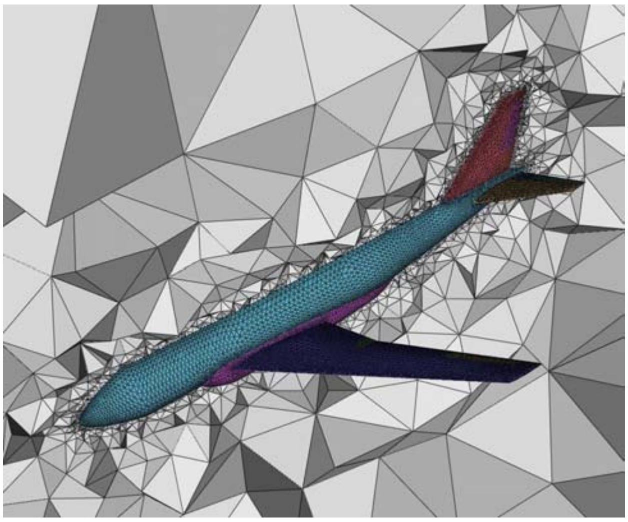

(b) SUMO mesh

Fig. 2 Representative geometry of the B747 model in SUMO

replacement of expensive experimental measurements.

The CEASIOM aerodynamic module, referred to as the Aerodynamic Model Builder (AMB), has functionality to allow the generation of tables of aerodynamic forces and moments required for flight dynamics analysis. The approach is to use sampling and data fusion to generate the tables, with a variety of sources of aerodynamic data. These aspects are now described.

4.1 Semi-Empirical Method

The Data Compendium (DATCOM) is a document of more than 1500 pages covering detailed methodologies for determining stability and control characteristics of a variety of aircraft configurations. In 1979, DATCOM was programmed in Fortran and renamed the USAF stability and control digital DATCOM . Digital DATCOM is a semi-empirical method which can rapidly produce the aerodynamic derivatives based on geometry details and flight conditions. DATCOM was primarily developed to estimate aerodynamic derivatives of conventional configurations [18, 19]. For a conventional aircraft, DATCOM gives all the individual components (body, wing, horizontal and vertical tail), and aircraft forces and moments. Digital DATCOM has been implemented in AMB. A DATCOM input file is produced by interpreting and formatting the XML aircraft data. In addition the flight conditions of interest are added to the DATCOM file.

4.2 Potential Solver

TORNADO [3], a Vortex Lattice Method (VLM), is an open source Matlab© implementation of a modified horse-shoe vortex singularity method for computing steady and low reduced frequency time-harmonic unsteady flows over wings. It can predict a wide range of aircraft stability and control aerodynamic derivatives [20]. The lifting surfaces are created as unions of thin, not necessarily flat, quadrilateral surface segments. Effects of airfoil camber are modeled by surface normal

[3] `www.redhammer.se/tornado/`

rotation. Leading edge control surfaces are modeled likewise. The modification to the horseshoe vortices allows trailing edge control surface deflection by actual mesh deformation. The steady wake can be chosen fixed in the body coordinate system or following the free stream. Overall effects of compressibility at high Mach number are assessed by the Prandtl-Glauert similarity role (see Anderson [21]), and zero-lift drag estimates are obtained by Eckert's flat plate analogy.

The fuselage might be modeled in the VLM using several techniques. The simplest approximation is modelling the aircraft fuselage as two flat elements with shapes corresponding to its planar projections. It is found [22] that for a generic aircraft configuration this model provides considerably different values of normal force and pitching moment coefficient slopes with respect to experimental results. One alternative consists in using the slender body theory developed by Munk [23]. The main assumption, which is met in traditional aircraft fuselage, is that the diameter of the body is far less than its length. However, some restrictions are connected to this theory, i.e. the body should have the shape of a body of revolution which is a condition met with difficulty in a real aircraft. Then, the fuselage surface can be modeled by a number of flat panels approximating its shape and the strength of sink/source distribution in each panel is the solution of a system of linear equations. This technique was tested for a three-dimensional representation of fuselage geometry [22] and is adopted herein. The basic flow solver is wrapped by user interfaces to create tables of aerodynamic coefficients and derivatives for export to flight simulators and flight control system design software. To calculate the first order derivatives, TORNADO performs a central difference calculation using the pre-selected state and disturbing it by a small amount. With the distorting wake, non-linear effects will be visible in some designs, especially in those where main wing/stabiliser interactions are important. The panelling for TORNADO is automatically produced within AMB from the XML geometry description.

4.3 Euler Solver

EDGE [4] is a parallelized CFD flow solver system for solving 2D/3D viscous/inviscid, compressible flow problems on unstructured grids with arbitrary elements [15]. EDGE can be used for both steady state and time accurate calculations including manoeuvres and aeroelastic simulations. The flow solver employs an edge-based formulation which uses a node-centered finite-volume technique to solve the governing equations. The control volumes are non-overlapping and are formed by a dual grid, which is computed from the control surfaces for each edge of the primary input mesh. In any Edge mesh, all the mesh elements are connected through matching faces. In the flow solver, the governing equations are integrated explicitly towards steady state with Runge-Kutta time integration. Convergence is accelerated using agglomeration multigrid and implicit residual smoothing. Time accurate computations can be performed using a semi-implicit, dual time stepping scheme which exploits convergence acceleration techniques via a steady state from inner iteration procedure. Several turbulence models [24, 25] are implemented in the solver.

A key feature in the present investigation is the analysis with deflected control surfaces. The way EDGE calculates the aerodynamics of control surface deflections is based on the use of transpiration boundary conditions. In this approach, instead of moving the grid, the wall velocity component normal to the actual deflected surface is prescribed. Such approach eliminates the need of mesh deformation, thus all calculations can be run virtually on the clean configuration grid, but on the other hand, this imposes a limitation on the amount of maximum and minimum deflections. An alternative approach would be the generation of a different grid for every new configuration of deflected control surfaces. This approach is not feasible for the intended use of creating aerodynamic tables given the number of possible combinations of control surfaces and corresponding

[4] `http://www.edge.foi.se/`

deflection angles.

In this paper, EDGE is used in Euler mode with pre-set reasonable values for the maximum and minimum deflection of each defined control surface. All calculations were obtained using one single grid generated with SUMO .

4.4 CFD Interface

A Matlab© graphical interface was developed to enhance the available aerodynamic sources included in the AMB, which were previously restricted to DATCOM and TORNADO . The CFD interface [26] is extremely general and flexible, as illustrated in Fig. 3. The interface preprocesses the flow of informations generated in the AMB module and creates suitable input files to the particular CFD solver used. The status of the job is monitored and when successfully finished, the CFD output is postprocessed and converted in a format fully compatible with the Stability and Control tools embodied in CEASIOM . The surface and flowfield solution are then translated in a format compatible with Tecplot ® [27]. The option of parallel calculation is available to reduce the overall computational time. The iterative process $AMB \rightarrow CFD \rightarrow AMB$ is likely to be repeated several times during the generation of aerodynamic tables. A second CFD code, in addition to EDGE , was interfaced to the AMB. This is the Parallel Multi-Block (PMB) solver, a research code under development at the University of Liverpool [28]. When the flow conditions feature the onset and development of vortical structures, shock-induced separation and other viscous-related phenomena, the task can be tackled using the RANS equations. The PMB solver can be used both in inviscid and viscous mode. The CFD interface has been tested extensively and used in several works [29, 30, 31].

A variety of calculations were obtained using the CFD interface, including the flow simulation around a fixed aircraft configuration with a generic deflection for any available control surface (i.e., landing configuration with deployment of multiple controls) and unsteady time-accurate analysis for the model undergoing forced harmonic motions in the three body axes for the prediction of dynamic derivatives.

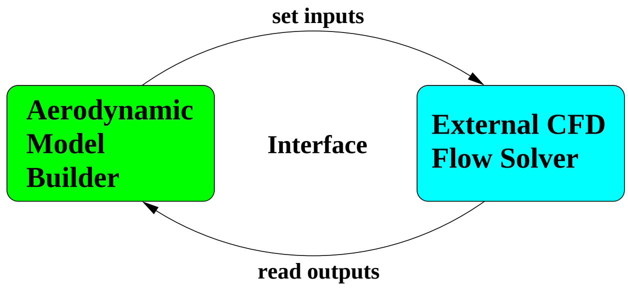

Fig. 3 Interfacing AMB to a generic CFD solver

4.5 Sampling and Data Fusion Methods

The application of the aerodynamic prediction methods in the current work is for the generation of tables of forces and moments. This potentially entails a large number of calculations, which will be a particular problem if CFD is the source of the data. This issue was addressed by sampling, reconstruction and data fusion in a previous work [32]. Two scenarios were postulated, based on a requirement for tables for a completely new design and for updating tables for existing designs which are being altered. Fig. 4 illustrates the sampling and data fusing algorithms.

In the first scenario it is assumed that the requirement is for a high fidelity model and that this can be generated offline (i.e. the calculation can be done overnight without a user waiting for the model during an interactive session). In this scenario the emphasis is on sampling finding nonlinearities in the forces and moments. Two approaches to this sampling, based on the Mean Squared Error criterion of Kriging and the Expected Improvement Function [33, 34], were considered [32]. The second scenario is when a designer is involved in an interactive session. It is assumed that the aircraft geometry is incremented from an initial design, perhaps selected from a library, and that a high fidelity model is available for the initial design from the first scenario. Data fusion (based on co-Kriging) is then used to update this initial model, based on a small number of calculations at an acceptable cost (which at present rules out RANS). In this

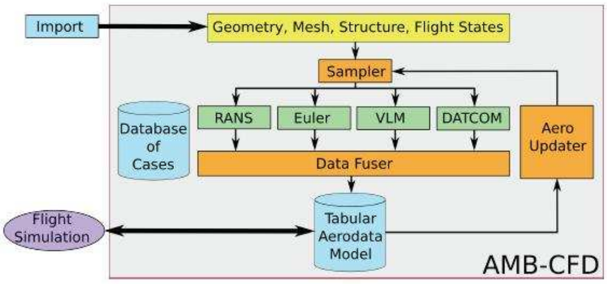

Fig. 4 CEASIOM framework system illustrating the sampling and data fusing algorithms

scenario it is assumed that the flow topology resulting from the initial geometry does not change during the geometry increments. If this is not the case (i.e., the wing sweep angle increases so that vortical flow starts to dominate at high angles), then either a new initial geometry needs to be selected, or the interactive session needs to be suspended so that a new high fidelity model can be generated under scenario one.

Using these techniques it was shown that tables could be generated in the order of 100 calculations under the first scenario and 10 calculations under the second scenario.

4.6 CEASIOM Aerodynamic Table Format

The aerodynamic model considered within the CEASIOM framework is tabular in form. The model consists of tables of forces and moments for a set of aircraft states and controls which span the flight envelope. The aerodynamic table consists of as many rows as the number of possible permutations of the aircraft states and controls, usually on the order of 10^3 or even 10^4 entries. Each entry in the table contains the 6 aerodynamic coefficients in wind axis as function of the states and controls. The aircraft states feature the angles of incidence (angle of attack, α, and sideslip, β), the Mach number, M, and the angular rates referred to the body axis, p, q and r, respectively, for the roll, pitch and yaw rates. CEASIOM was actively developed to handle unconventional configurations with multiple control surfaces [9], enhancing the traditional aerodynamic model based on three conventional control surfaces (ailerons, rudder and elevator). A variable number of columns in the table is reserved to accommodate the aircraft controls.

On the order of tens of CFD calculations are required to fill-in the aerodynamic tables for the static dependencies due to the angles of incidence and the deflection of control surfaces. A challenging task is the computation of the dynamic dependencies of the aerodynamic loads on the angular rates. Several options were investigated. Quasi-steady dynamic derivatives can be obtained with DATCOM or, on the next level of fidelity, TORNADO . Although cheap to compute, the validity of these estimations is the primary concern when analyzing critical flow conditions and unconventional configurations. CFD has the potential to provide accurate predictions of dynamic derivatives. The accuracy retained in the solution is obtained at the price of large requirements in terms of computational time and resources. Unsteady time-accurate solutions with grid deformation at each physical time step to conform the applied harmonic motion are typically on the order of hundreds times more expensive than a steady state solution. A well-established framework was presented in Da Ronch et al. [35] for the estimation of dynamic derivatives using time-accurate solutions. Nonetheless, the described approach is not a viable option in the design phase and for the present study. A valid alternative to the time-marching method is offered by the Harmonic Balance (HB) method where the non-linear CFD solution is truncated up to a predescribed number of Fourier modes. As demonstrated in Da Ronch et al. [36], two harmonics are generally adequate to predict dynamic derivatives even at critical flow conditions. Compared to the CPU time required for an unsteady time-accurate solution, the solution obtained using the HB method is on the order of tens times faster [37], and about 3 to 4 times more expensive than a steady state analysis. This option is of interest to fill-in the aerodynamic tables.

The approach followed in this study uses TORNADO for the prediction of quasi-steady dynamic derivatives. This was considered a reasonable approximation because the interest is on the linear and quasi-linear aerodynamics. At higher Mach numbers, compressibility effects can be significant. However, the range in the angle of attack at cruise speed is limited to about 6.0°. The idea of exploiting the potential of the HB approach was not adopted because this method was implemented within the structured framework of the PMB solver. All the CFD-based calculations herein included were obtained using the unstructured EDGE solver.

5 The FCSDT module

The Flight Control System (FCS) is a multidisciplinary design space that involves control effector sizing and topology, as well as the systems architecture that actuates these effectors. The Flight Control System Designer Toolkit (FCSDT) is a software framework to develop flight control systems. The environment integrates modules to address each of the aforementioned design streams. The module Flight Control System Architecture (FCSA) is used to develop the effector topology and systems architecture. This environment enables the user to edit the control effector topology, by adding and removing effectors, in addition to design of the systems architecture for each respective effector. The Stability and Control Analyser Assessor (SCAA) module implements the aerodynamic data from the AMB into a Simulink® flight mechanics model, which is then used to analyse the aircraft flight dynamics. Analysis variables include the trim values, associative linear results (which include time and frequency domain results) and simulation results. This module also includes an Eigen structure assignment algorithm, for design of a state feedback controller. Eigen structure assignment is a control synthesis method which the input is a desired Eigen structure, or Eigen vectors and values, specifying the reduced state and control input matrices and control structure. The output is the control gains that yield the desired Eigen structure. More details on the mechanics of Eigen structure assignment algorithm can be found in Liu and Patton [38]. There is an additional control design environment in LTIS, which uses H_∞ control synthesis to generate a robust feedback controller.

6 B747 Model Example

The Boeing 747 is a very large four-engined turbofun transport aircraft designed to ferry more than 350 passengers on medium–long haul flights, which includes transatlantic operations. The aircraft, designed in the 1960s to meet growth demands for mass long haul transport, has spanned several decades of operations, and is still in service today. The aircraft surviving several generations has spawned a number of derivatives with varying operational requirements. The Boeing 747-100 employs a large number of individual control surfaces, beyond the conventional elevator, ailerons and rudder.

To obtain the necessary low speed characteristics the wing has triple–slotted trailing flaps and Krueger leading edge flaps. The Krueger flaps outboard of the inboard nacelle are variable cambered and slotted while the inboard Krueger flaps are standard unslotted. Longitudinal control is obtained through four elevator segments and a movable stabilizer. The lateral control employs five spoiler panels, an inboard aileron between the inboard and outboard flaps, and an outboard aileron which operates with flaps down only on each wing. The five spoiler panels on each wing also operate symmetrically as speedbreaker in conjunction with the most inboard sixth spoiler panel. Directional control is obtained from two rudder segments [39]. An aircraft model using a model generated for the Boeing 747-100 has been selected for investigation of its flight dynamics within FCSDT. This is to validate FCSDT for use on multiple surface aircraft examples. The geometry of the B747 model is represented in Fig. 5 for different fidelity-level approximations. The simplest approximation of the model, which is suitable for VLM-based calculations, consists of the lifting surfaces only. The TORNADO geometry is shown in Fig. 5(a). Lifting surfaces were sized to closely match the B747 geometry and its control surfaces. Comparison between the

TORNADO geometry and the B747 geometry of the real aircraft, as illustrated in Fig. 6, shows that the simplified model reproduce well the main features of the model geometry. Then, the baseline geometry was enhanced to include the influence of the fuselage which is modelled as a slender body in TORNADO calculations. The corresponding geometry is illustrated in Fig. 5(b). Lifting surfaces were not modified to accommodate the fuselage. On the top of the fidelity–stair, the watertight geometry used in CFD calculations shown in Fig. 5(c) was generated with SUMO . The surface geometry was simplified by removing the engine nacelles and adopting a simple representation of the fairings. These were considered reasonable simplifications because the interest is on the flow development on the upper lifting surfaces.

Both TORNADO and EDGE geometries consist of control surfaces which were sized from the aircraft model, including the inner and outer ailerons, all-movable stabilizer, two–segment elevator and two–segment rudder. These control surfaces are highlighted in Fig. 5(c).

Details of the surface grid are shown in Fig. 7. The surface mesh does not conform to hinge lines, but surface elements affected by the rotation are mapped into the CFD solver EDGE , and these are coloured. The geometry has sharp trailing edges which are adequate for inviscid flow models. For a RANS model, the proper modelling of trailing edges of lifting surfaces is required. Also, a detailed RANS model would include the resolution of the opening gaps and exposed edges of a deflected control device.

6.1 Validation of Aerodynamic Sources

This section summarizes predictions of aerodynamic loads based on several aerodynamic options with wind tunnel experimental data provided by the manufacturer [1]. At low speed, predictions obtained with TORNADO are considered. At higher speed featuring compressibility effects and formation of shock waves, low–order and CFD-based results are presented.

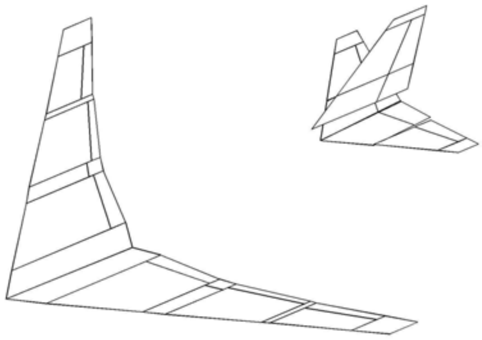

(a) TORNADO geometry

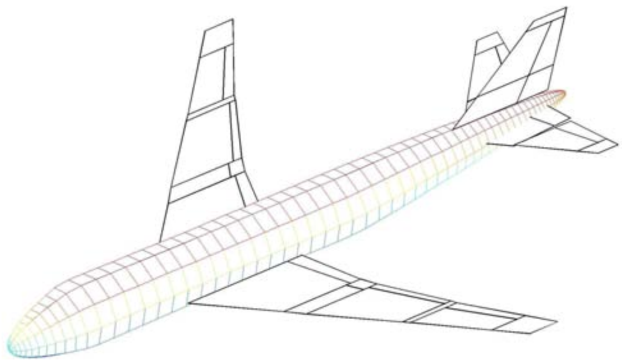

(b) TORNADO geometry with fuselage

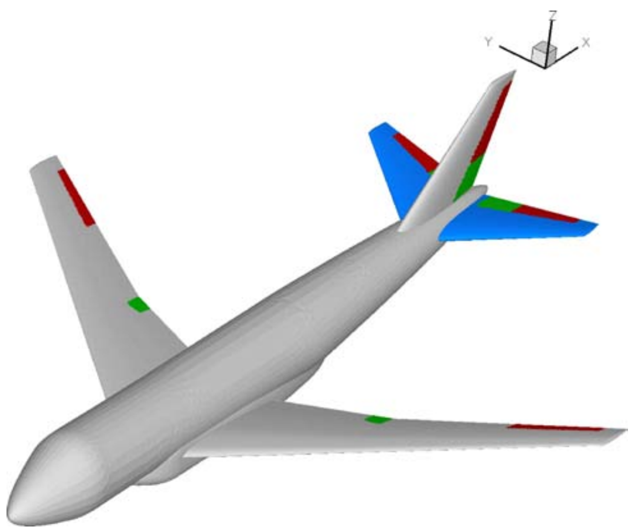

(c) Watertight geometry for CFD analysis

Fig. 5 Geometry of the B747 model for several aerodynamic options for increasing fidelity

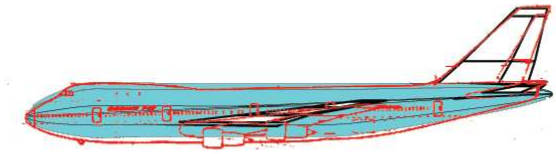

(a) Side view

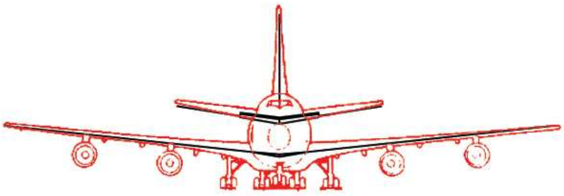

(b) Front view

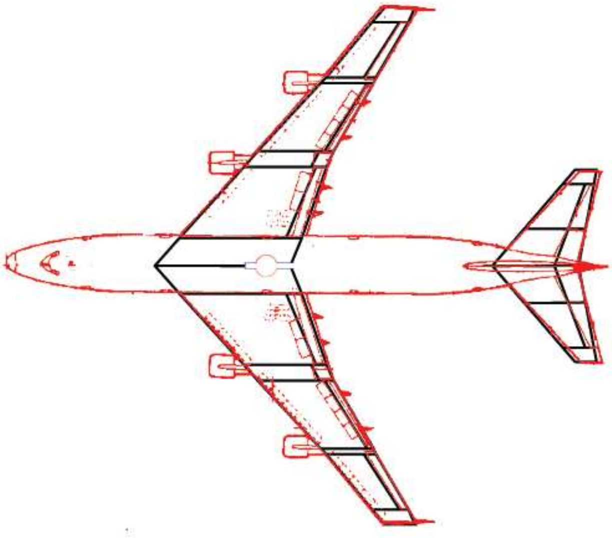

(c) Top view

Fig. 6 Comparison of the TORNADO geometry in Fig. 5(a) with a three-view drawing of the B747 model

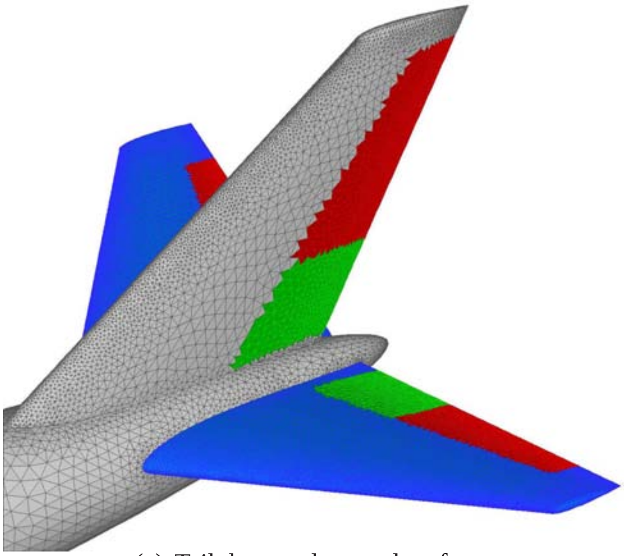

(a) Tailplane and control surfaces

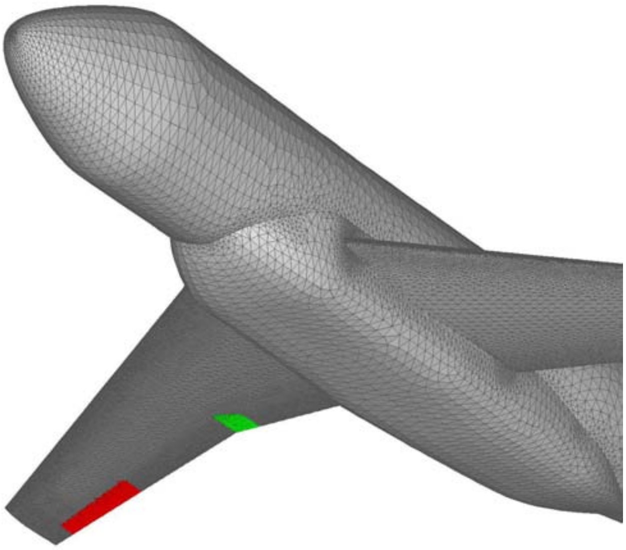

(b) Fairings and control surfaces on main wing

Fig. 7 Surface mesh for the B747 model

6.1.1 Low Speed Aerodynamics

Predictions of lift and pitching moment coefficients are illustrated in Fig. 8. A significant change in the force slope is observed between 10.0° and 15.0° in the experimental data set. The moment coefficient is also non-linear above the static stall. Numerical predictions of the lift coefficient in Fig. 8(a) were obtained with TORNADO . The data set labelled as "TORNADO Baseline" is based on the original formulation of the VLM, which predicts a linear increase in the aerodynamic coefficients for increasing angle of attack. Then, the option to account for a viscous correction was switched on and the corresponding data set is referred to as "TORNADO Viscous". The stall prediction is based on informations of $dC_L/d\alpha$ and C_{L0}. The two numerical data sets start to diverge at around 10.0°, with the viscous calculation underpredicting the static stall. Fig. 8(b) illustrates for the pitching moment coefficient the effect of modelling the fuselage with sink/source singularities in the TORNADO calculations. The resulting effect of including the fuselage is to offset the data set obtained for the Wing-Vertical-Horizontal tail "WVH" configuration (see Fig. 5(a) for the geometry) by a certain amount. Although the overall agreement is improved over the range in the angle of attack for the Fuselage-Wing-Vertical-Horizontal tail "FWVH" configuration (see Fig. 5(b) for the geometry), a poorer agreement is achieved at low angles of attack.

One example describing the authority of the control surfaces deflection is provided in Fig. 9. Numerical calculations were obtained using TORNADO with the viscous correction switched off and the clean configuration of lifting surfaces. The outboard elevator was deflected. The comparison between numerical and experimental data sets is reasonable. The slope of the force coefficient is slightly underpredicted, while a good prediction is provided for the moment coefficient.

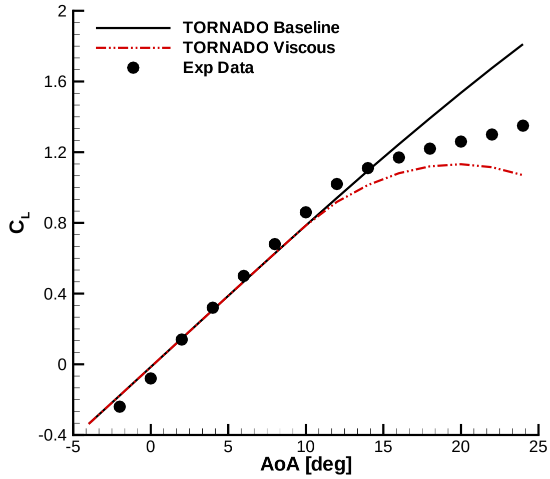

(a) Lift coefficient

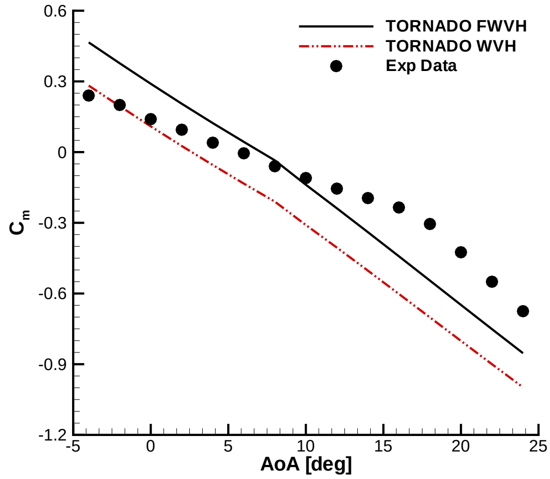

(b) Pitching moment coefficient

Fig. 8 Prediction of lift and pitching moment coefficients for several values of angle of attack at Mach number of 0.15

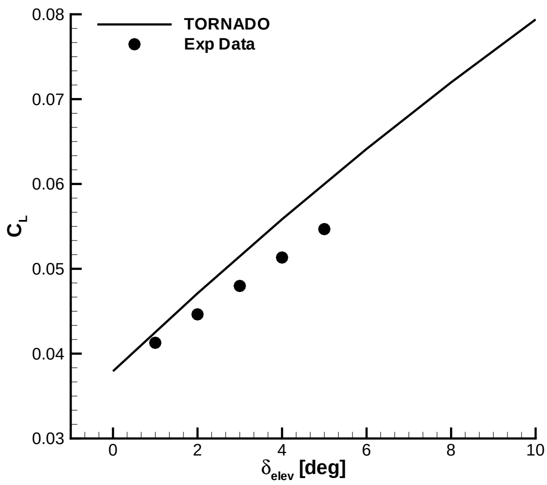

(a) Lift coefficient

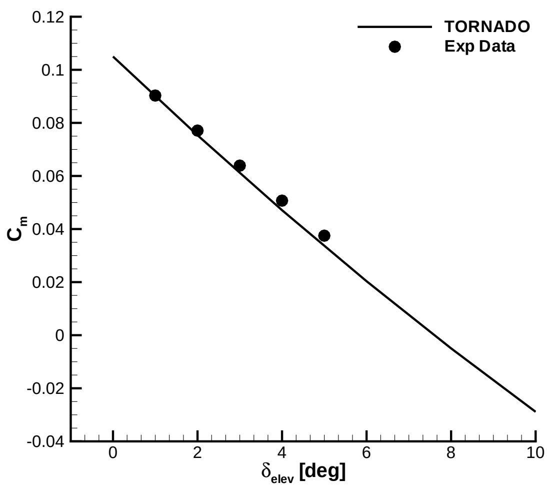

(b) Pitching moment coefficient

Fig. 9 Prediction of lift and pitching moment coefficients for several values of outboard elevator deflection at Mach number of 0.15

6.1.2 High Speed Aerodynamics

Fig. 10 shows the lift curve slope produced by the various fidelity-level aerodynamic codes. The Euler results show the closest correlation to the Boeing 747-100 published data. The actual values and the curve slope are compare well to experimental values. DATCOM shows comparable lift-curve slope, with the actual values slightly less than experimental data. However, as Mach number increases, DATCOM results begin to fall away from experimental results. TORNADO results without compressibility correction remain constant through all Mach numbers, and the offset from experimental data increases because the more influential effect of compressibility at higher speeds. TORNADO results with the Prandtl-Glauert similarity role overpredict the lift-curve slope, diverging at higher Mach numbers. A reason for the poor correlation to experimental data is likely to be caused by the simple compressibility correction which begins to break down at the higher end of the transonic regime.

Fig. 11 shows the drag polars computed by the various codes at the Mach numbers specified. It is observed that DATCOM result shows the best correlation with the NASA experimental data. This is not unexpected because DATCOM was developed using conventional configurations and the semi-empirical methods calibrated using, among others, the Boeing 747. Thereby, the parasitic drag term, C_{D0}, is estimated using parameters such as wetted area. The Euler results differ from the viscous experimental data in the absence of any estimation of the drag due to friction. As the angle of attack is increased, drag divergence is predicted. TORNADO results achieve a poor agreement with other data sets.

Fig. 12 illustrates the pitching moment coefficient for several values of the angle of attack, which is a good indicator for the aircraft static stability. At lower Mach numbers, a good correlation of numerical data sets is achieved in terms of stability. However, the numerical values deviate by a constant offset, which suggests dis-

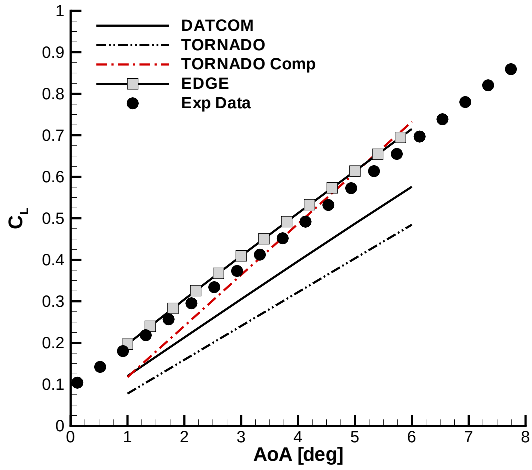

(a) $M = 0.75$

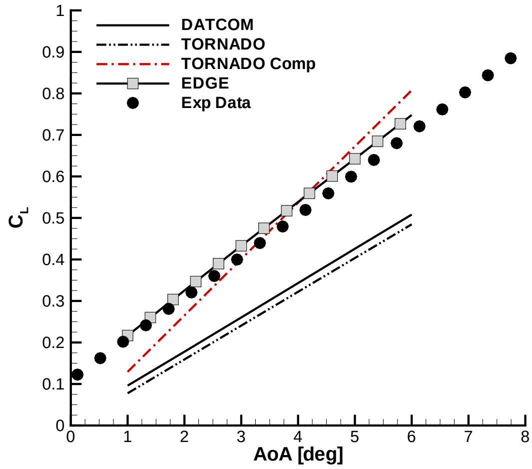

(b) $M = 0.80$

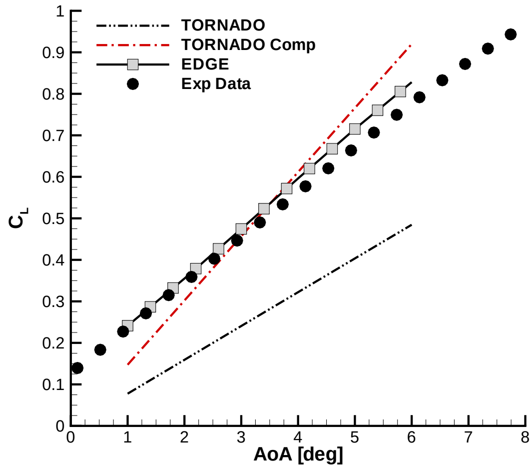

(c) $M = 0.85$

Fig. 10 Prediction of lift coefficient for several values of angle of attack in transonic regime

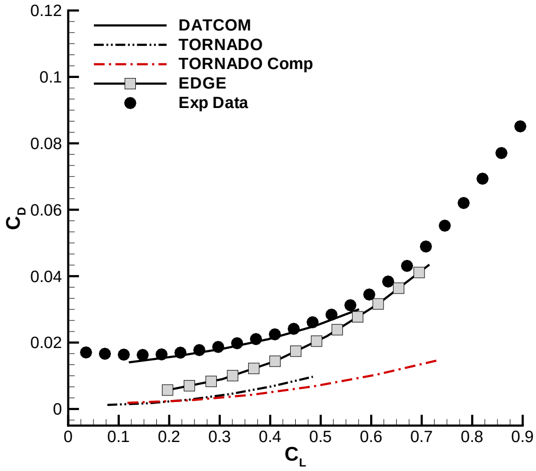

(a) $M = 0.75$

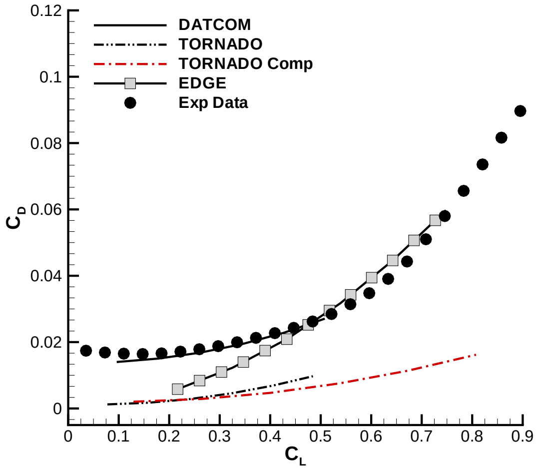

(b) $M = 0.80$

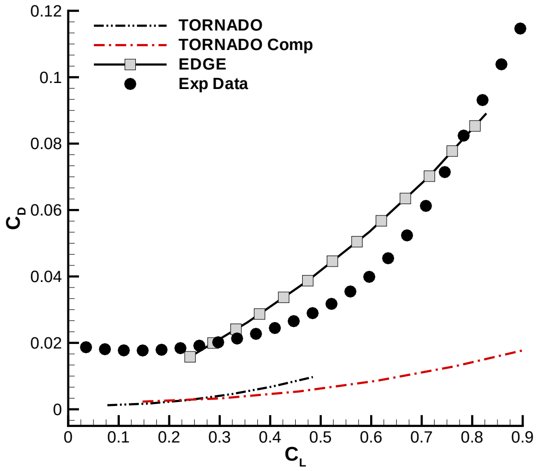

(c) $M = 0.85$

Fig. 11 Prediction of lift versus drag coefficient in transonic regime crepancies in the C_{m0} value. This is expected because the term is highly dependent on the airfoil section and fuselage geometry used in the computations. TORNADO with compressibility correction overpredicts the curve-slope, amplifying the compressibility effect on the static stability. The Euler results achieve a good comparison with experimental data for the Mach numbers considered. At this point the trend line for the experimental data set has non-linear behaviour, the static stability migrating toward neutral stability. This could be attributed to an effect associated to non-linear effects induced by viscous phenomena.

The overall performance of the Euler results is satisfactory and shows the need of using CFD to obtain good predictions in the transonic regime, where results based on traditional methods become suspect.

The surface pressure distribution on the B747 model is illustrated in Fig. 13 for several flow conditions and geometry configurations. These test cases were taken from the database of CFD calculations that were run for the generation of look-up tables. A solution obtained on the clean configuration is depicted in Fig. 13(a) at angle of incidence of 6.0° and Mach number of 0.8. A strong shock wave forms on the upper main wing and extends downstream until 50% of the local chord, not interacting with the control surfaces. The remaining two subfigures were obtained for the same flow conditions, i.e., angle of incidence of 1.0° and Mach number of 0.9, but for different geometry configurations. The control sign convention adopted within CEASIOM framework is as defined by Cook [40], which is a positive control surface displacement gives rise to a negative aeroplane response. Fig. 13(b) shows the solution obtained imposing a positive deflection to the four elevator segments (trailing-edge down). A shock wave appears near the hinge axis where the flow suddenly expands to conform to the control deflection. The two rudder segments were deflected by a negative angle (trailing-edge starboard) in the solution illustrated in Fig. 13(c). The resulting flow is locally accelerated near the rudder hinge line.

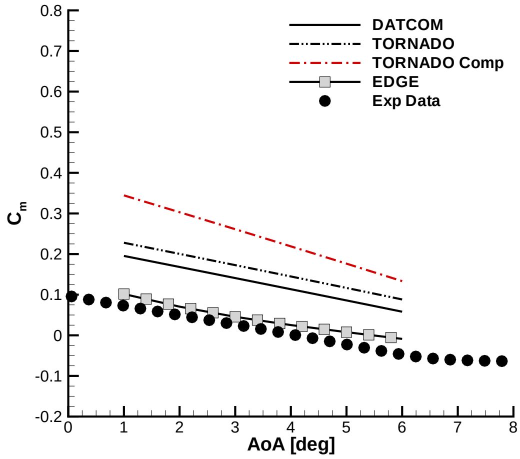

(a) $M = 0.75$

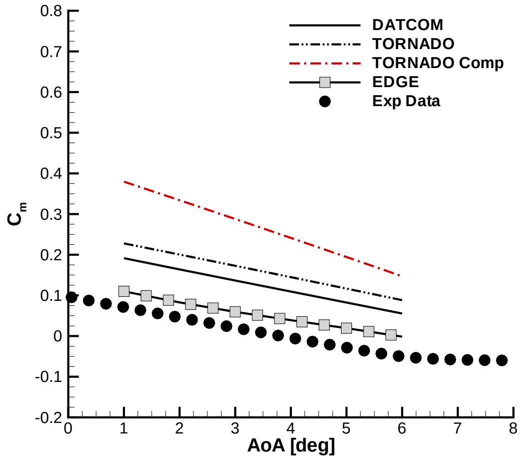

(b) $M = 0.80$

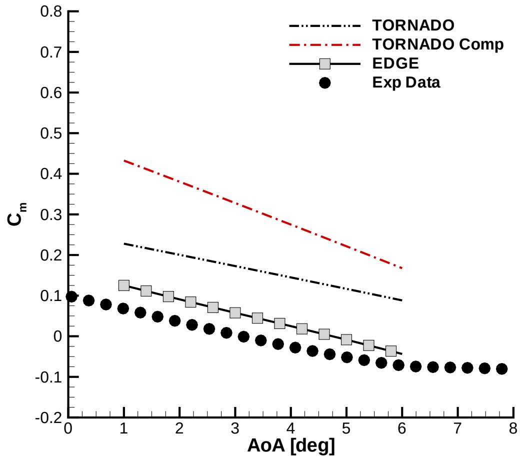

(c) $M = 0.85$

Fig. 12 Prediction of pitching moment coefficient for several values of angle of attack in transonic regime

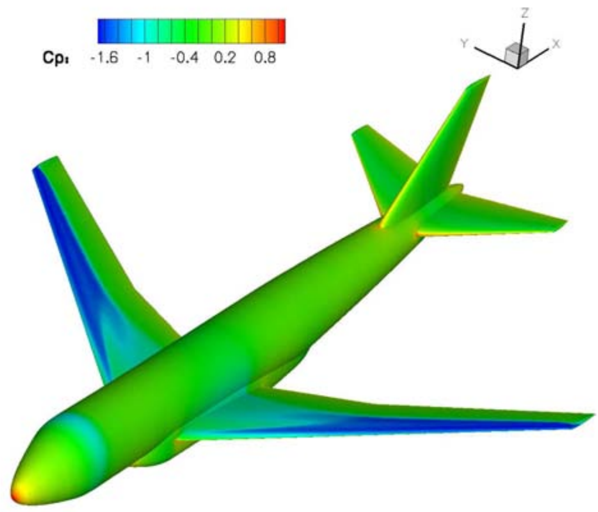

(a) $M = 0.8$, $\alpha = 6.0°$

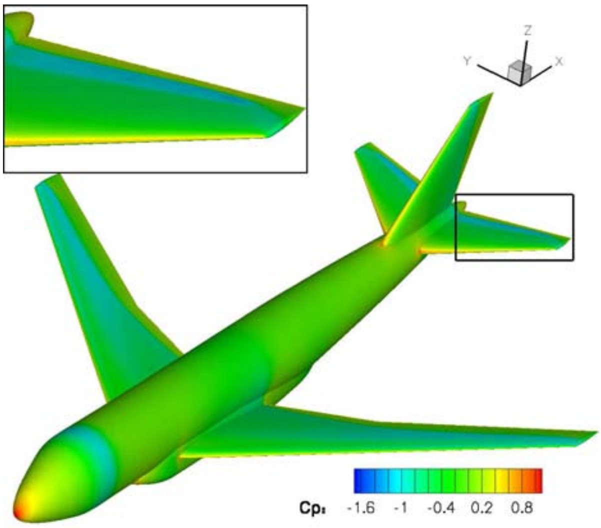

(b) $M = 0.9$, $\alpha = 1.0°$, positive elevator deflection

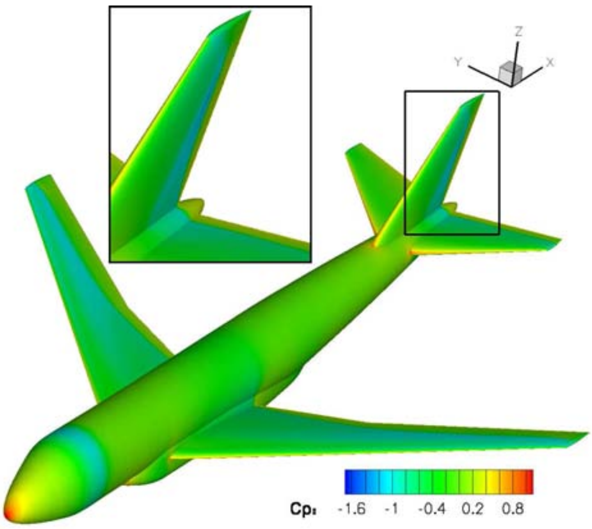

(c) $M = 0.9$, $\alpha = 1.0°$, negative rudder deflection

Fig. 13 Surface pressure distribution for the B747 model geometry at several angles of attack, α, Mach numbers, M, and configurations

6.2 Stability Analysis

The non-linear set of equations governing the rigid aircraft motion are first linearized with respect to an equilibrium (trim) point. The solution of a standard eigenvalue problem, expressed in the classical form $(\mathbf{A} - \lambda \mathbf{I})\, x$, is solved for the eigenvalues, λ_i, and corresponding eigenvectors, x_i. The modes of motion are then identified in an automatic way from the solution of the eigenvector problem, though the identification might fail when eigenvalues are non-conjugate for some modes. The identified modes for the B747 example are illustrated in Fig. 14.

The short period mode is characterized by rapid oscillations in angle of attack about a nearly constant flight path. This mode can be excited by rapidly deflecting the elevator, and usually it is fast and well damped. In simulated flight it can be excited by initial disturbance in pitch rate. The time to halve the motion amplitude is plotted against the period of oscillation in Fig. 14(a). Numerical results are overplotted to ICAO recommendations.

The phugoid mode is characterized by very slow oscillations in pitch angle and velocity, and a nearly constant angle of attack. To excite this mode, the airplane should be trimmed in level flight and next stick should be pulled back slightly and maintained. This pitches the airplane up into a climb. As the airplane climbs, it loses speed and lift, causing it to gradually pitch downward and enter a dive. During the dive, the airplane gains speed and lift, bringing it back into a climb. The main aerodynamic forces taking part in inducing a phugoid are lift and drag forces. The lift is the oscillation inducer and the drag is a damper. The phugoid period is illustrated in Fig. 14(b).

The Dutch-roll mode is moderately involving fast side-to-side swaying of the aircraft. It involves oscillations in bank, yaw, and sideslip angles. In a flight-state display, a Dutch roll will be indicated by the velocity vector circle oscillating from side to side. This mode can be excited by rapidly deflecting the rudder, and should be fast and well damped. In simulated flight it can be excited by initial disturbing of sideslip angle. Numerical results for the Dutch-roll mode are shown in Fig. 14(c).

6.3 Linear Model Analysis

Fig. 15 presents the trimmed values for the angle of incidence and elevator angle. In general, as Mach number increases, the required angle of incidence decreases, and the required elevator angle increases. This suggests that a lower angle of incidence is required for the required C_L, primarily generated by the main lifting surface, the elevator angle providing the necessary pitching moment to balance the aircraft. This also implies that the pitching moment generated by the elevators, with little influence on the lift. DATCOM results suggest that the influence of the elevators is significant on the vehicular lift, leading to a smaller efficiency value or C_L/C_m.

Fig. 16 shows the pole plots generated. It is difficult to interpret these without also inspecting the eigen vectors in tandem. The figure primarily shows the differences in the higher frequency modes, and will be the focus of this brief discussion. The SCAA module, using a function to compare the eigen vectors, identifies the higher frequency complex poles as the short period, with the relatively lower frequency poles as the Dutch-roll. The results show large discrepancies with correlation of the TORNADO result with compressibility effect showing the greatest difference in short period prediction. The migration with Mach number all suggest a similar trend of increasing natural undamped frequency.

However, these can all be made to behave dynamically, within the linear region, similar to one another. The control synthesis method, eigen structure assignment, is used to compute gain values for a feedback controller. The values computed specify a eigen value of $-2 \pm 2i$ for the short period mode, for a feedback controller $A + BK$. A and B are known, plant and control matrix, respectively. Fig. 17 shows the variations in feedback gain values using the available aerodynamic sources. K_α refers to the gain value of feedback angle of attack to elevator, and K_q is

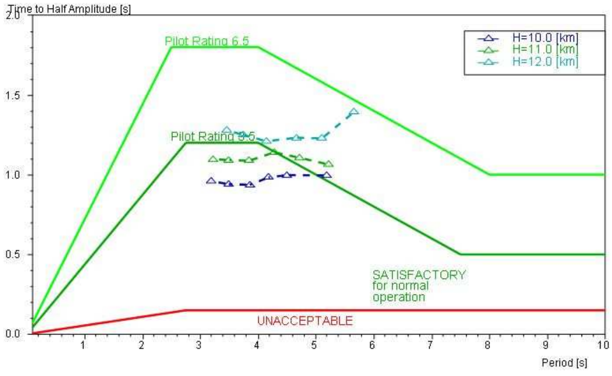

(a) Short period characteristics

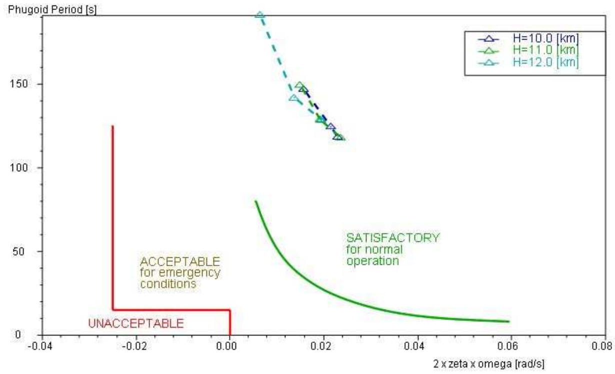

(b) Phugoid characteristics

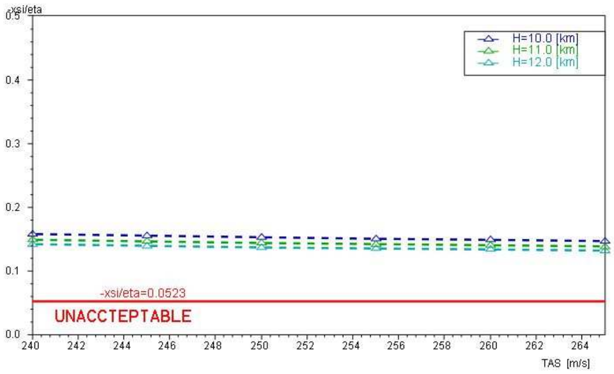

(c) Dutch roll characteristics

Fig. 14 Flight dynamic properties of the B747 aircraft at cruise speed

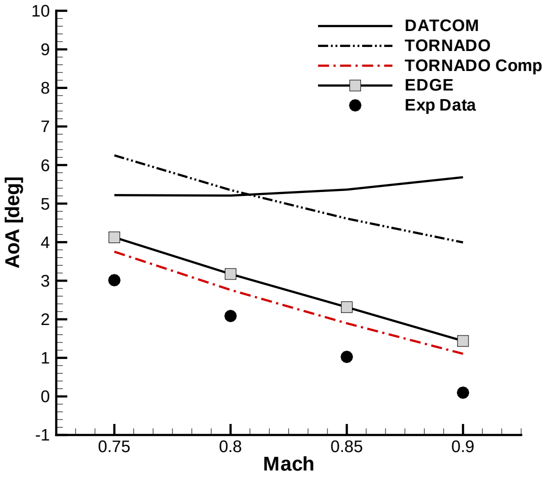

(a) Angle of attack

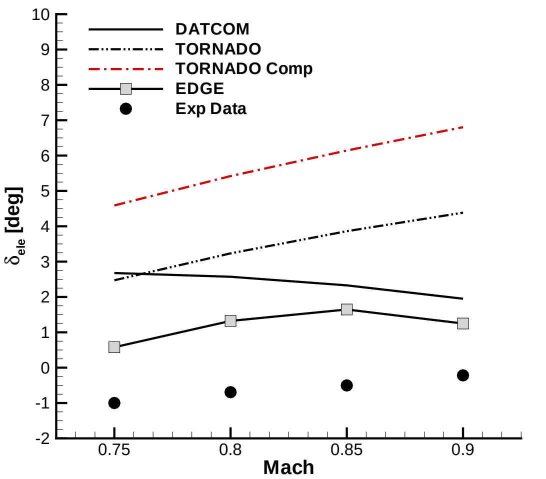

(b) Elevator deflection

Fig. 15 Trimmed angle of incidence and elevator angles

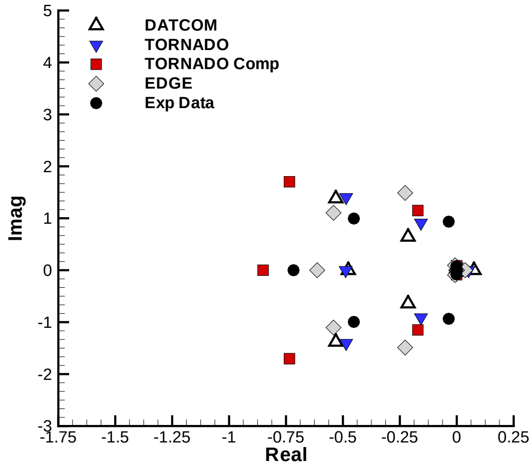

(a) $M = 0.75$

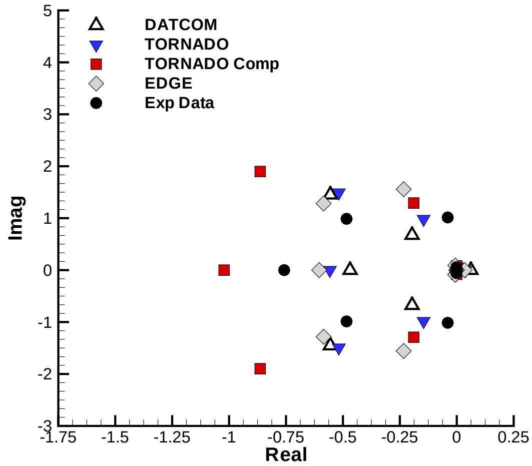

(b) $M = 0.80$

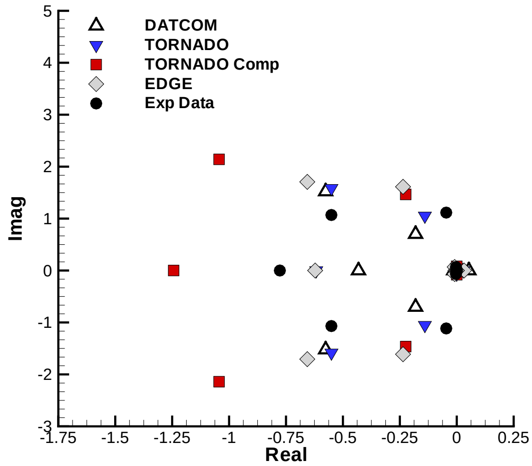

(c) $M = 0.85$

Fig. 16 Pole plots for various angles of attack

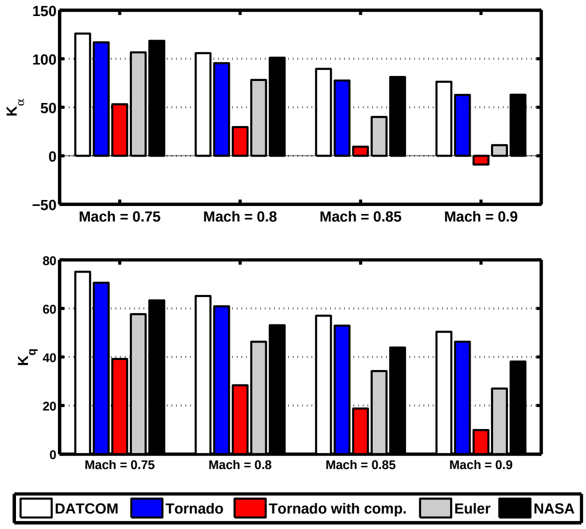

Fig. 17 Feedback gain values computed by Eigen Structure Assignment control synthesis

the pitch damping, or pitch rate feedback to elevator. This can similarly be used to specify the complete eigen structure, limited by the number of inputs available.

6.4 Single Rudder Surface Failure

The following brief example models a rudder failure of a single rudder surface, at an altitude of 11000 *m* and a range of Mach numbers. The trim is obtained by computing the required angle of incidence and bank angle states for steady state constant altitude and velocity. This is achieved through computing the required throttle, elevators, ailerons and rudder, where the bottom surfaces is failed and stuck at -10.0°. Fig. 18 shows the state values and the computed input values. The top-left subfigure plots the angle of attack in solid line and the roll angle in dashed line.

Fig. 19 presents the pole plot for this failure case. The traditional complex modes of short period, phugoid and dutch roll can be readily identified. However, it is not easy to automatically identify these by way of an algorithm, as cross coupling, or involvement of states that are not typically associated to these modes is observed. The dynamics of the longitudinal complex modes also observes lateral modes and visa

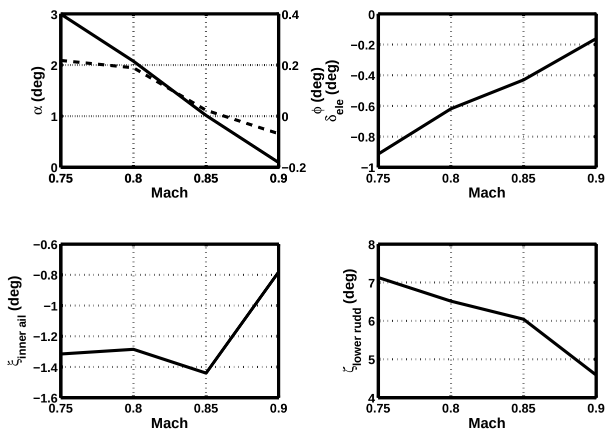

Fig. 18 Trim values computed for Boeing 747-100 with failed lower rudder at -10.0°

versa. This leads to behaviour in the short period and phugoid, where variations in roll and yaw occur, where the Dutch-roll might now have a little pitching motion.

For each of these conditions, it would be possible to generate a controller to remove abnormal behaviour, and return the modes to more traditional modes. This would make the aircraft behave with normal handling in the event of failures. Such a comprehensive controller is seldom designed due to the large number of flight configurations, conditions and failure modes. Robust controllers are preferable, where a limited number of controllers are designed, for a complete flight envelope. A tool built by TsAGI for FCSDT integrates such a design tool, which uses H_∞ control synthesis to design robust controllers.

7 Conclusions

Recent advances in the generation of aerodynamic tables for flight dynamics are described in this paper using the CEASIOM software, which was developed within the frame of the SimSAC Project, Simulating Aircraft Stability And Control Characteristics for Use in Conceptual Design, sponsored by the European Commission 6th Framework Programme. Aerodynamic tables in tabular form were generated using several aero-

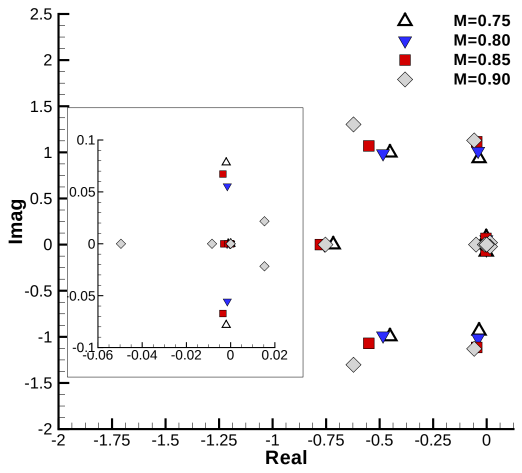

Fig. 19 Pole plot for the Boeing 747-100 with failed lower rudder at -10.0°

dynamic codes, from semi-empirical and linear potential methods to CFD. A smart procedure was considered to fuse data obtained with different fidelity-level aerodynamics. A database was then generated for low and high speed aerodynamics. The test case is the Boeing 747-100. The study demonstrates the establishment of a robust and automated procedure, with the aircraft geometry description defined using on the order of hundreds of parameters as the starting point and the look-up aerodynamic tables based on Euler calculations as the ending point. This chain embodies major achievements. The automated generation of volume unstructured grids stems from the aircraft geometry description. This step is automated, not requiring user's intervention in most of the cases. Realistic control surfaces system was sized based on the aircraft geometry model and included in all numerical models. Parallel CFD calculations can be routinely launched to fill-in aerodynamic tables. Aircraft states and controls are selected within the flight envelope in an efficient manner, with the benefit of reducing the total number of CFD analysis. This step is also automated. The user can define deliberately additional critical flow conditions to analyze in case the sampling algorithm failed to resolve important non-linear features in aerodynamic loads.

Using the aerodynamic database, the trim solution was computed for the different aerodynamic sources. In transonic regime with compressibility effects and formation of shock waves, the Euler results were in agreement with experimental data. Eigen values were calculated for several Mach numbers and results were compared to experimental data, demonstrating the need of CFD to complement low-order methods. A feedback controller was designed using the eigenstructure assignment to migrate the poles to a specified location. Then, a case with a failed lower segment rudder was examined. A new trim condition was found and pole plots presented for several Mach numbers.

8 Acknowledgments

The financial support by the European Commission through co-funding of the FP6 project SimSAC is gratefully acknowledged.

9 Copyright Statement

References

[1] Rodney, C. H. and Nordwall, D. R., "The Simulation of a Jumbo Jet Transport Aircraft. Volume II. Modelling Data (B747)," The Boeing Company, Wichita Division, 1970.

[2] Von Kaenel, R., Rizzi, A., Oppelstrup, J., Grabowski, T., Ghoreyshi, M., Cavagna, L., and Bérard, A., "CEASIOM: Simulating Stability & Control with CFD/CSM in Aircraft Conceptual Design," *26th International Congress of the Aeronautical Sciences, ICAS*, 2008.

[3] Rizzi, A., “Modeling and Simulating Aircraft Stability & Control – the SimSAC Project,” *AIAA Guidance, Navigation and Control Conference*, AIAA–2010–8238, Toronto, Ontario, 2010.

[4] Ghoreyshi, M., Vallespin, D., Da Ronch, A., and Badcock, K. J., “Simulation of Aircraft Manoeuvres Based on Computational Fluid Dynamics,” *AIAA Guidance, Navigation and Control Conference*, AIAA–2010–8239, Toronto, Ontario, 2010.

[5] Dul, F. A., Grabowski, T., and Stefanek, L., “Implementation of the Basic Linear Quadratic Gaussian Control within the Flight Control System,” SimSAC Official Deliverable, D 5.3-1, 2008.

[6] Grabowski, T. G., Mieszalski, D., and Marcinkiewincz, E., “Stability Analysis in Conceptual Design Using SDSA Tool,” *AIAA Guidance, Navigation and Control Conference*, AIAA–2010–8242, Toronto, Ontario, 2010.

[7] Da Ronch, A., “GUESS: Generic Unknown Estimator for Aircraft Structural Sizing,” Master Thesis, Royal Institute of Technology (KTH), Stockholm, Sweden, October 2008.

[8] Cavagna, L., Ricci, S., and Travaglini, L., “NeoCASS: an Integrated Tool for Structural Sizing, Aeroelastic Analysis and MDO at Conceptual Design Level,” *AIAA Guidance, Navigation and Control Conference*, AIAA–2010–8241, Toronto, Ontario, 2010.

[9] McFarlane, C., Richardson, T. S., Da Ronch, A., and Badcock, K. J., “Comparison of Conventional and Asymmetric Aircraft Configurations Using CEASIOM,” *AIAA Guidance, Navigation and Control Conference*, AIAA–2010–8243, Toronto, Ontario, 2010.

[10] Maheri, A., “Designer Decision Support System (DDSS) Development and Overview,” SimSAC Official Deliverable, D 5.3-3, 2010.

[11] Dawes, W. N., Dhanasekaran, P. C., Demargne, A. A. J., Kellar, W. P., and Savill, A. M., “Reducing Bottlenecks in the CAD-to-Mesh-to-Solution Cycle Time to Allow CFD to Participate in Design,” *Journal of Turbomachinery*, Vol. 123, No. 3, 2001, pp. 552–557.

[12] Hahn, A. S., “Vehicle Sketch Pad: A Parametric Geometry Modeler for Conceptual Aircraft Design,” 48th AIAA Aerospace Sciences Meeting, Orlando, Florida, January 2010. AIAA 2010-657.

[13] Eller, D., “Mesh Generation Using SUMO and TetGen,” SimSAC Official Deliverable, D 2.3-5, 2009.

[14] Si, H., “On Refinement of Constrained Delaunay Tetrahedralizations,” In Proceedings of the 15th International Meshing Roundtable, September 2006. Software available from `http://tetgen.berlios.de`, July 2009.

[15] Eliasson, P., “EDGE, a Navier-Stokes Solver for Unstructured Grids,” FOI Report, FOI–R–0298–SE, 2005.

[16] Eliasson, P., Vos, J. B., Da Ronch, A., Mengmeng, Z., and Rizzi, A., “Virtual Aircraft Design of TransCRuiser – Computing Break Points in Pitch Moment Curve,” *28th AIAA Applied Aerodynamic Conference*, AIAA–2010–4366, 2010.

[17] Tomac, M., Rizzi, A., and Oppelstrup, J., “From Geometry to CFD Grids - An Automated Approach for Conceptual Design,” AIAA Guidance, Navigation and Control Conference, AIAA-2010-8240, 2-5 August 2010, Toronto, Ontario.

[18] Razgonyaev, V. and Mason, W. H., “An Evaluation of Aerodynamic Prediction Methods Applied to the XB-70 for Use in High Speed Aircraft Stability and Control System Design,” 33rd Aerospace Sciences Meeting and Exhibit, AIAA95-0759, Reno, Nevada, 1995.

[19] Williams, J. E. and Vukelich, S. R., “The USAF Stability and Control Digital DATCOM,” McDonnell Douglas Astona UTICS Company, St Louis Division, St Louis, Missouri, 63166, 1979, AFFDL-TR-79-3032.

[20] Melin, T., “TORNADO: a Vortex–Lattice MATLAB Implementation for Linear Aerodynamic Wing Applications,” Master Thesis, Royal Insitute of Technology (KTH), Department of Aeronautics, Sweden, December, 2000.

[21] Anderson, J. D., “Modern Compressible Flow,” McGraw Hill, 1990.

[22] Khrabrov, A., Kolino, K., Glazkov, S., Sidoryuk, M., Bolyrev, S., and Anoshin, J., “Review of Steady and Unsteady Panel Codes and Tier I Simulation of Aircraft Stability and Control

Characteristics Using Vortex Lattice Method," SimSAC Official Deliverable, D 3.2-1, 2007.

[23] Munk, M., "The Aerodynamic Forces on Airship Hull," NACA Report No. 184, 1924.

[24] Wallin, S. and Johansson, A. V., "An Explicit Algebraic Reynolds Stress Model for Incompressible and Compressible Turbulent Flows," *Journal of Fluid Mechanics*, Vol. 403, 2000, pp. 89–132.

[25] Hellsten, A., "New Advanced $k-\omega$ Turbulence Model for High Lift Aerodynamics," *AIAA Journal*, Vol. 43, No. 9, 2005, pp. 1857–1869.

[26] Da Ronch, A., "CFD Start Documentation," SimSAC Official Deliverable, D 3.2-6, 2009.

[27] "Tecplot. User's Manual. Version 10," Amtec Engineering, Inc., Bellevue, Washington, September 2003.

[28] Badcock, K. J., Richards, B. E., and Woodgate, M. A., "Elements of Computational Fluid Dynamics on Block Structured Grids using Implicit Solvers," *Progress in Aerospace Sciences*, Vol. 36, 2000, pp. 351–392.

[29] Da Ronch, A., Ghoreyshi, M., Badcock, K. J., Mengmeng, Z., Oppelstrup, J., and Rizzi, A., "On Time Optimal Manoeuvres of Aicraft Using CFD–Based Tabular Data with Multiple Control Surfaces," Abstract Submitted to the 49th AIAA Aerospace Science Meeting, 4–7 January 2010, Orlando, FL.

[30] Ghoreyshi, M., Da Ronch, A., Badcock, K. J., Dees, J., Bérard, A., and Rizzi, A., "Aerodynamic Modelling for Flight Dynamics Analysis of Conceptual Aircraft Designs," 27th AIAA Applied Aerodynamics Conference, AIAA-2009-4121, 22-25 June 2009, San Antonio, TX.

[31] Ghoreyshi, M., Badcock, K. J., Da Ronch, A. Marques, S., Swift, A., and Ames, N., "Framework for Estabilishing the Limits of Tabular Aerodynamic Models for Flight Dynamics Analysis," Presented as AIAA-2009-4121, Under Review for Publication in Journal of Aircraft.

[32] Ghoreyshi, M., Badcock, K. J., and Woodgate, M. A., "Accelerating the Numerical Generation of Aerodynamic Models for Flight Simulation," *Journal of Aircraft*, Vol. 46, No. 3, 2009, pp. 972–980.

[33] Lophaven, S. N., Nielsen, H. B., and Søndergaard, J., "DACE, A Matlab Kriging Toolbox. Version 2.0," Technical Report IMM-TR-2002-12, Technical University of Denmark, August 1, 2002.

[34] Lophaven, S. N., Nielsen, H. B., and Søndergaard, J., "Aspects of the Matlab Toolbox DACE," Technical Report IMM-REP-2002-12. Technical University of Denmark, August 1, 2002.

[35] Da Ronch, A., Vallespin, D., Ghoreyshi, M., and Badcock, K. J., "Computation of Dynamic Derivatives Using CFD," *28th AIAA Applied Aerodynamics Conference*, AIAA–2010–4817, Chicago, IL, 2010.

[36] Da Ronch, A., Ghoreyshi, M., Badcock, K. J., Görtz, S., Widhalm, M., Dwight, R. P., and Campobasso, M. S., "Linear Frequency Domain and Harmonic Balance Predictions of Dynamic Derivatives," *28th AIAA Applied Aerodynamic Conference*, AIAA–2010–4699, Chicago, IL, 2010.

[37] Mialon, B., Khrabrov, A., Da Ronch, A., Cavagna, L., Mengmeng, Z., and Ricci, S., "Benchmarking the Prediction of Dynamic Derivatives: Wind Tunnel Tests, Validation, Acceleration Methods," *AIAA Guidance, Navigation and Control Conference*, AIAA–2010–8244, Toronto, Ontario, 2010.

[38] Liu, G. P. and Patton, R. J., "Eigenstructure Assignment for Control System Design," Wiley, 1998.

[39] Heffley, R. K. and Jewell, N. F., "Aircraft Handling Qualities Data," NASA CR 2144, Dec. 1972.

[40] Cook, B. H., "Flight Dynamics Principles," Butterworth Heinemann, Cranfield, 1997.